

Estimates of phonon-mediated electron-electron scattering rates in the metal elements

K. Schwartzman*

Department of Physics, Indiana University, Indiana, Pennsylvania 15705

W. E. Lawrence†

Department of Physics, Ohio State University, Columbus, Ohio 43210

(Received 23 December 1992)

Starting with an exact expression for the quasiparticle decay rate due to the phonon-mediated electron-electron interaction, we derive a simple approximate formula for the magnitude of its T^2 coefficient at low temperatures. Comparison with measured decay rates in Cd and several nonmagnetic transition metals yields agreement to within at worst a factor of 2. Similar agreement holds for estimated electrical resistivities.

I. INTRODUCTION

The electron-phonon and Coulomb interactions give rise in ordinary metals to two nearly distinct scattering mechanisms, electron-electron scattering (due to a combination of the Coulomb interaction and the exchange of *virtual* phonons^{1,2}) and electron-phonon scattering (referring to the emission and absorption of *real* phonons). As long as phonons are well-defined excitations, as is certainly the case for the elementary metals, the distinction between these two mechanisms is sharp.³ Clear signatures exist in the asymptotic temperature dependences of the quasiparticle decay rate in normal metals, as is well known: Electron-phonon scattering produces cubic temperature dependence far below the Debye temperature $T \ll \Theta_D$, and linear dependence above. Electron-electron scattering produces quadratic dependence both far below and above Θ_D , but with different coefficients in the two regimes because only the Coulomb interaction contributes at higher temperatures. Similar signatures are associated with the electrical resistivity, with “cubic” replaced by “ T^5 ”. Only a limited amount of data relating to electron-electron scattering exist in elementary metals because electron-phonon scattering dominates it at all but very low temperatures.

There are several theoretical approaches to quasiparticle decay rates or transport coefficients that incorporate phonon-mediated electron-electron scattering. The earliest treatments¹⁻³ showed how processes attributable to both real and virtual phonons are included in the familiar Dyson’s equations of the coupled electron-phonon system. Later treatments^{4,5} combined the Coulomb and phonon-mediated interactions within a Fermi liquid formalism⁶ to construct the full Landau scattering function. Still later treatments⁷⁻⁹ obtained the full scattering function and real phonon processes from the three self-energy diagrams of Fig. 1.

Among these theoretical works, only Refs. 4 and 5 arrive at quantitative results and compare these with experiment. The current state of agreement between theory and experiment is discussed in a detailed review of electron-electron scattering by Kaveh and Wisner.¹⁰ A

briefier discussion is given in a more general review of transport properties by van Vucht, van Kempen, and Wyder.¹¹ To summarize briefly, calculations are performed for the alkali metals³ (except for Li), the noble metals, Al, and Pb.⁴ The phonon-mediated interaction has been detected experimentally only in the low-temperature electrical resistivities of K (Refs. 12 and 13) and Al (Refs. 14 and 15) among these metals. In Al, the theory and experiment agree within 50%, which is within the accuracy of the resistivity calculation. In K, the calculated resistivity exceeds experiment by about a factor of 3. This calculation is more accurate than the Al one, and the reason for the discrepancy is not known. In the other alkali metals (those that do not undergo Martensitic phase transformations), electron-electron scattering is detectable only at high temperatures,^{16,17} where only the Coulomb interaction contributes. The agreement here with Na, K, Rb, and Cs is within 40%. Electron-electron scattering is detectable in the noble metals at both low¹⁸⁻²⁰ and high²¹ temperatures, but the Coulomb interaction always dominates so that the phonon-mediated

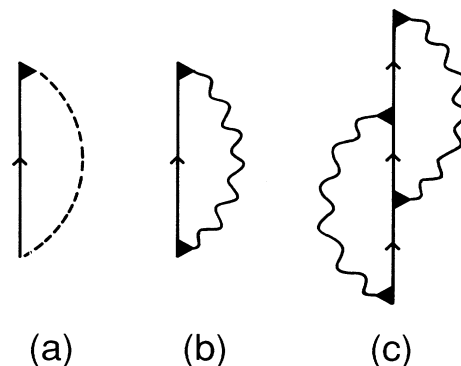


FIG. 1. The three quasiparticle self-energy diagrams used in Ref. 9 to obtain the total inelastic decay rate. Solid and wavy lines represent the renormalized quasiparticle and phonon propagators, respectively, the dashed line is the bare Coulomb interaction, and triangles are the screened, Coulomb-corrected vertices.

part is unresolvable. The calculated magnitudes exceed experiment by about a factor of three in all cases.

Electron-electron scattering is not seen in Pb because the electron-phonon contribution swamps it above the superconducting transition $T > T_c = 7.2$ K. It is interesting, though, that MacDonald⁴ finds the phonon-mediated interaction much stronger than the Coulomb interaction in the superconducting metals Al and Pb. In the alkali metals, the Coulomb interaction is stronger in absolute terms, but the phonon-mediated interaction wins out in the electrical resistivity because it has more umklapp character.⁵

There is evidence of electron-electron scattering in the transition metals, but existing theoretical treatments account only for the Coulomb interaction.^{22,23} These will be discussed later in connection with present results. We will describe in Sec. II an approximation for the phonon-mediated interaction that applies in principle to any ordinary metal. The approximation relies heavily on connections with empirically determined parameters and avoids assumptions relating specifically to Fermi surface shape or band structure. On the other hand, we do not believe that the Coulomb interaction can be incorporated realistically at a similar level of approximation. We compare in Sec. III with experimental data in nonmagnetic metals whose electron-phonon coupling is sufficiently strong that phonon-mediated scattering could dominate or at least compete with Coulomb scattering. We will argue that W is a borderline case with $\lambda \sim 0.3$ (about twice the value found in most alkali metals).²⁴ It is encouraging that Al easily satisfies this condition⁴ even though (with $\lambda = 0.43$) (Ref. 24) it is still in the weak-coupling regime. The comparison of theory and experiment focuses on quasiparticle decay rates which provide the most direct test, and includes the electrical resistivity at a more qualitative level. Conclusions are summarized in Sec. IV. The simple formula which we will derive seems to be accurate to within a factor of two, and it gives a consistent account of electron-electron scattering in the nonmagnetic transition metals as well as in the simple metals Cd and Al.

II. DERIVATION OF APPROXIMATE DECAY RATE FORMULA

This section forms an extension of the general formulation for inelastic decay rates developed in Ref. 9. As an introductory step we obtain a simplified expression (but still exact, within Migdal's theorem) for the low-temperature limit, i.e., the coefficient of T^2 , arising from

$$\text{Im}\Sigma_d(\mathbf{k}, \epsilon) = 2\pi \int_0^\infty \omega d\omega [2n(\omega) + f(\omega - \epsilon) + f(\omega + \epsilon)]$$

$$\times \sum_{\mathbf{q}} \sum_{\mathbf{p}} \delta(Z\epsilon_{\mathbf{k}-\mathbf{q}}) \delta(Z\epsilon_{\mathbf{p}}) \delta(Z\epsilon_{\mathbf{p}+\mathbf{q}}) \left| \sum_{\sigma} g_{\sigma}(\mathbf{k}-\mathbf{q}, \mathbf{k}) D_{\sigma}(\mathbf{q}, \omega) g_{\sigma}(\mathbf{p}+\mathbf{q}, \mathbf{p}) \right|^2 \quad (1)$$

and

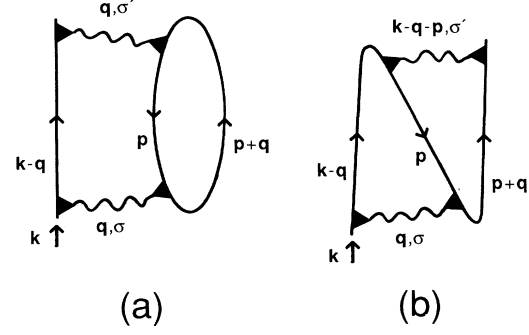


FIG. 2. (a) and (b) Effective diagrams representing $\text{Im}\Sigma$ as given by Eqs. (1) and (2), respectively. It is understood that vertices are Coulomb renormalized, but only the explicit particle lines are cut in forming the imaginary part.

the phonon-mediated interaction. We then proceed to develop an approximation.

A. Exact low-temperature form

Diagrams of Fig. 1 have the following interpretations when the imaginary parts are taken to compute the decay rate: The third diagram, usually neglected on the grounds of Migdal's theorem,² was shown by Lopes dos Santos and Sherrington⁷ to represent the exchange contribution to phonon-mediated electron-electron scattering. The second diagram represents not only real phonon processes but also direct phonon-mediated electron-electron scattering (through the finite phonon linewidth),¹⁻³ and the interference between Coulomb and phonon-mediated scattering amplitudes (through the dynamics of its vertices).⁹ This interference causes the partial cancellation which becomes complete in the jellium model.²⁵

We showed in Ref. 9 that both electron-electron and electron-phonon mechanisms are given correctly to lowest order in the phonon linewidths by calculating the imaginary part (only) of the quasiparticle self-energy from the *effective* diagrams of Fig. 2, in which the vertices are taken static. The Coulomb interaction (ignored here) is included simply by making each interaction line a sum, as described in Ref. 9. Clearly the direct and exchange virtual phonon-mediated contributions are represented by Figs. 2(a) and 2(b), and real phonon contributions arise as resonances in Fig. 2(a). The expressions are

$$\begin{aligned}
\text{Im}\Sigma_{\text{ex}}(\mathbf{k}, \epsilon) = & -\pi \int_0^\infty d\omega [n(\omega) + f(\omega - \epsilon)] \int_0^\infty d\omega' [f(\epsilon - \omega' - \omega) - f(\epsilon - \omega')] \\
& \times \sum_{\mathbf{q}} \sum_{\mathbf{p}} \delta(Z\epsilon_{\mathbf{k}-\mathbf{q}}) \delta(Z\epsilon_{\mathbf{p}}) \delta(Z\epsilon_{\mathbf{p}+\mathbf{q}}) \\
& \times \sum_{\sigma} g_{\sigma}(\mathbf{k}-\mathbf{q}, \mathbf{k}) D_{\sigma}^*(\mathbf{q}, \omega) g_{\sigma}(\mathbf{p}+\mathbf{q}, \mathbf{p}) \\
& \times \sum_{\sigma'} g_{\sigma'}(\mathbf{p}+\mathbf{q}, \mathbf{k}) D_{\sigma'}(\mathbf{k}-\mathbf{p}-\mathbf{q}, \omega') g_{\sigma'}(\mathbf{k}-\mathbf{q}, \mathbf{p}), \quad (2)
\end{aligned}$$

where n and f are Bose and Fermi functions, respectively, $D_{\sigma}(\mathbf{q}, \omega)$ is the phonon propagator, and $g_{\sigma}(\mathbf{k}-\mathbf{q}, \mathbf{k})$ are the electron-phonon vertex functions attached to the ends of it in Fig. 2. The combination $g D g$ is the ω -dependent phonon-mediated scattering amplitude. We follow the notation of Ref. 9 except in the choice of arguments of the vertex functions. It is preferable here to choose the outgoing and incoming electron momenta rather than the average and the difference; Table I provides translation between this and the convention of Ref. 9. The physical (renormalized) quasiparticle energies are denoted by $\epsilon_{\mathbf{k}}$, so that $Z\epsilon_{\mathbf{k}}$ is unrenormalized, with Z the quasiparticle renormalization function $Z(\epsilon)$ evaluated at $\epsilon=0$. The delta functions therefore simply reduce the momentum sums to Fermi surface integrals; for example,

$$\sum_{\mathbf{p}} \delta(Z\epsilon_{\mathbf{p}}) = N(0) \quad (3)$$

is the unrenormalized density of one-spin states at the Fermi level.

The decay rate of a quasiparticle in state \mathbf{k} is

$$\tau^{-1}(\mathbf{k}) = \frac{2}{Z(\epsilon_{\mathbf{k}})} \text{Im}\Sigma(\mathbf{k}, \epsilon_{\mathbf{k}}). \quad (4)$$

For $T \ll \Theta_D$ only the low- ω limit of the phonon propagators $D_{\sigma}(\mathbf{q}, \omega) \rightarrow -2/\omega_{\mathbf{q}\sigma}$ is sampled, and the double frequency integral in Eq. (2) reduces to the single one in Eq. (1), which is equal to $\frac{1}{2}[\epsilon_{\mathbf{k}}^2 + (\pi k_B T)^2]$, the result for ordinary potential scattering. By taking this (static D_{σ}) limit we have eliminated the electron-phonon decay mechanism. It is convenient to average the decay rate over the Fermi surface, with the result

$$\begin{aligned}
\tau^{-1}(0) = & \frac{1}{N(0)} \sum_{\mathbf{k}} \tau^{-1}(\mathbf{k}) \delta(Z\epsilon_{\mathbf{k}}) \\
= & \frac{4\pi^3 (k_B T)^2}{N(0)Z(0)} \sum_{\mathbf{k}} \sum_{\mathbf{q}} \sum_{\mathbf{p}} \delta(Z\epsilon_{\mathbf{k}}) \delta(Z\epsilon_{\mathbf{k}-\mathbf{q}}) \delta(Z\epsilon_{\mathbf{p}}) \delta(Z\epsilon_{\mathbf{p}+\mathbf{q}}) \\
& \times \sum_{\sigma} g_{\sigma}(\mathbf{k}-\mathbf{q}, \mathbf{k}) \omega_{\mathbf{q}\sigma}^{-1} g_{\sigma}(\mathbf{p}+\mathbf{q}, \mathbf{p}) \\
& \times \sum_{\sigma'} [2g_{\sigma'}(\mathbf{k}-\mathbf{q}, \mathbf{k}) \omega_{\mathbf{q}\sigma'}^{-1} g_{\sigma'}(\mathbf{p}+\mathbf{q}, \mathbf{p}) - g_{\sigma'}(\mathbf{p}+\mathbf{q}, \mathbf{k}) \omega_{\mathbf{k}-\mathbf{p}-\mathbf{q}, \sigma'}^{-1} g_{\sigma'}(\mathbf{k}-\mathbf{q}, \mathbf{p})] \\
= & \tau_d^{-1}(0) + \tau_{\text{ex}}^{-1}(0). \quad (5)
\end{aligned}$$

The factor in square brackets identifies the direct and exchange contributions arising from Eqs. (1) and (2), respectively. In comparing with experimental results, it is usually appropriate to average also over the quasiparticle energy, $\tau^{-1} = \int d\epsilon (-\partial f / \partial \epsilon) \tau^{-1}(\epsilon)$, which is easily seen from the above-noted energy dependence to be related to the value at the Fermi level [Eq. (5)] by

$$\tau^{-1} = \frac{4}{3} \tau^{-1}(0), \quad (6)$$

also $\sim T^2$ at low temperatures. This result is exact (within Migdal's theorem, as generalized by Ref. 7) for the phonon-mediated electron-electron interaction at

TABLE I. Notation of Ref. 9 and the present work are compared for the electron-phonon vertex function [whose arguments correspond to the lower left vertices in Figs. 2(a) and 2(b)], and two self-energy contributions. The superscript (ii) refers to the purely phonon-mediated contribution to the imaginary part of the diagram in Fig. 1(b). This table is intended primarily for readers of Ref. 9.

	Reference 9	present work
vertex function	$g_{\sigma}(\mathbf{k}-\frac{1}{2}\mathbf{q}, \mathbf{q})$	$g_{\sigma}(\mathbf{k}-\mathbf{q}, \mathbf{k})$
contributions to $\text{Im}\Sigma$	$\text{Im}\Sigma_{1\phi}^{(ii)}$	$\text{Im}\Sigma_d$
	$\text{Im}\Sigma_{2\phi}$	$\text{Im}\Sigma_{\text{ex}}$

$T \ll \Theta_D$.

Equations similar to (1) and (2) were derived by Lopes dos Santos and Sherrington,⁷ although $\text{Re}D$ appears in place of D , which accounts for only half the contribution from real phonon emission and absorption.⁹ Equation (5) is equivalent to formulas used in Ref. 5 to compute the electrical and thermal resistivities in the alkali metals. The main difference between this and Refs. 4 and 5 is not in the description of the underlying phonon-mediated interaction, but in the nature of the approximations used to extract quantitative results. We now turn to the problem of obtaining quantitative estimates from Eq. (5).

B. Approximation

An approximate analytical formula was derived in Ref. 9 using a familiar set of assumptions, namely a spherical Fermi surface, Debye phonons, and jellium matrix elements. It is possible to derive an equally simple but more accurate result for the phonon-mediated part of the electron-electron interaction without these separate assumptions, but rather just a single one that specifies how the effective interaction is distributed over phonon states (i.e., the Brillouin zone). Allen and Silbergli³ derived a similar result using an "extended Debye model" for the phonon linewidth and spectral distribution function in evaluating Fig. 1(b). The main virtue of these treatments may be that the phonon linewidths (or similar quantities) incorporate the necessary integrals over the exact Fermi surface. To show this as simply as possible, consider the phonon linewidth due to the creation of electron-hole pairs²⁶

$$\gamma_{q\sigma} = 2\pi\omega_{q\sigma} \sum_{\mathbf{p}} |g_{\sigma}(\mathbf{p}+\mathbf{q}, \mathbf{p})|^2 \delta(Z\epsilon_{\mathbf{p}}) \delta(Z\epsilon_{\mathbf{p}+\mathbf{q}}). \quad (7)$$

The sum is over all pairs of states lying on the Fermi surface that are separated by \mathbf{q} . Umklapp processes are included most simply by drawing the Fermi surface in the repeated zone scheme as shown in Fig. 3. According to Eq. (7),

$$\sum_{\sigma} \gamma_{q\sigma} / \omega_{q\sigma}^2 = 2\pi \sum_{\mathbf{p}} \sum_{\sigma} \frac{|g_{\sigma}(\mathbf{p}+\mathbf{q}, \mathbf{p})|^2}{\omega_{q\sigma}} \delta(Z\epsilon_{\mathbf{p}}) \delta(Z\epsilon_{\mathbf{p}+\mathbf{q}}). \quad (8)$$

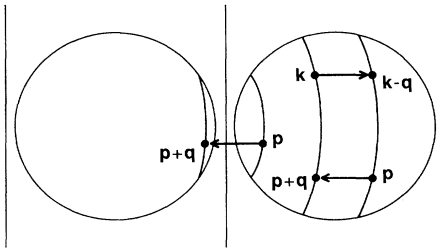


FIG. 3. Cylindrical sections of the Fermi surface represent the domain of \mathbf{k} and \mathbf{p} sums at fixed \mathbf{q} , as occur for example in Eqs. (5) and (7), with umklapp processes included by using the repeated zone scheme. A spherical Fermi surface is sketched for clarity only; the analysis is not restricted to this case.

Comparing this with the direct contribution τ_d^{-1} in Eq. (5), it is apparent that if g_{σ} is independent of \mathbf{k} (which refers to the azimuthal position on the cylinder in Fig. 3), then

$$\tau_d^{-1} = \frac{8\pi(k_B T)^2}{3N(0)Z(0)} \sum_{\mathbf{q}} \left[\sum_{\sigma} \gamma_{q\sigma} / \omega_{q\sigma}^2 \right]^2. \quad (9)$$

The scattering geometry on the Fermi surface, including Umklapp, has been treated exactly, in principle. The only real approximation involves the integrand in Eq. (9). It is shown in the Appendix that the *exact* τ_d^{-1} may be written in only slightly less transparent form and computed with essentially no greater difficulty. However, Eq. (9) is more useful for proceeding analytically.

To this end, we compare Eq. (9) with a similar expression for the average electron-phonon interaction strength λ . Microscopically,

$$\lambda_{\mathbf{k}} = Z(\mathbf{k}, 0) - 1 = 2 \sum_{\mathbf{k}'} \sum_{\sigma} \frac{|g_{\sigma}(\mathbf{k}, \mathbf{k}')|^2}{\omega_{\mathbf{k}-\mathbf{k}', \sigma}} \delta(Z\epsilon_{\mathbf{k}}) \quad (10)$$

is the quasiparticle renormalization parameter for a state \mathbf{k} in the Fermi surface, and λ is the Fermi surface average

$$\lambda = \frac{2}{N(0)} \sum_{\mathbf{k}} \lambda_{\mathbf{k}} \delta(Z\epsilon_{\mathbf{k}}).$$

If we write λ as a double integral and integrate over \mathbf{k} holding $\mathbf{q} = \mathbf{k} - \mathbf{k}'$ fixed, then according to Eq. (7),

$$\lambda = \frac{1}{\pi N(0)} \sum_{\mathbf{q}} \sum_{\sigma} \gamma_{q\sigma} / \omega_{q\sigma}^2, \quad (11)$$

an identity derived by Allen.²⁶ The \mathbf{k}' sum may be replaced by a Brillouin-zone sum because umklapp processes are counted in the \mathbf{k} sum, as required by the definition of $\gamma_{q\sigma}$ [Eq. (7)]. A comparison of Eqs. (9) and (11) shows that $\tau_d^{-1} \sim \lambda^2 / (1 + \lambda)$ with a coefficient that depends only on the functional form of the quantity

$$Q(\mathbf{q}) = \sum_{\sigma} \gamma_{q\sigma} / \omega_{q\sigma}^2 \quad (12)$$

defined within the Brillouin zone. Specifically, we can write

$$\tau_d^{-1} = \frac{8\pi^3 N(0) \lambda^2 (k_B T)^2}{3n_{\text{ion}} (1 + \lambda)} C[Q(\mathbf{q})], \quad (13)$$

where the dimensionless functional C is

$$C[Q(\mathbf{q})] = \sum_{\mathbf{q}} Q^2(\mathbf{q}) \left[\sum_{\mathbf{q}} Q(\mathbf{q}) \right]^{-2} \sum_{\mathbf{q}} 1 \quad (14)$$

and $n_{\text{ion}} = \sum_{\mathbf{q}} 1$ is the density of primitive cells, or in cases studied here simply the density of ions.²⁷

Now C is uniquely minimized by the constant function, for which it takes the value $C_{\text{min}} = C[\text{constant}] = 1$. A more physically realistic choice is however $Q(\mathbf{q}) \sim 1/q$, because this is the exact behavior at small q . Therefore we adopt the value

$$C[1/q] = \frac{4}{3} \quad (15)$$

which is close to C_{\min} . Since the actual function $Q(\mathbf{q})$ is anisotropic, we suspect that C is greater than $\frac{4}{3}$. Pronounced phonon softening would also be expected to enhance C .

The exchange counterpart τ_{ex}^{-1} cannot be reduced to an expression like Eq. (9) without a stronger approximation than the one used there; in this case we simply note that if the combination $\sum_{\sigma} g_{\sigma} \omega_{\sigma}^{-1} g_{\sigma}$ is independent of \mathbf{q} (as well as of the other momentum arguments), then the remaining steps follow as before, with the result

$$\tau_{\text{ex}}^{-1} = -\tau_d^{-1}/2. \quad (16)$$

We adopt this approximation because of its simplicity, and we also note that it represents the maximum value of $|\tau_{\text{ex}}^{-1}|$ (see Appendix), and thus underestimates the total rate τ^{-1} .

The final approximate result may be written conveniently in terms of experimentally determined parameters,

$$\tau^{-1} \approx \frac{16\pi^3 N(0)\lambda^2}{9n_{\text{ion}}(1+\lambda)} (k_B T)^2 = \frac{8\pi}{3} \gamma_{\text{el}} \left[\frac{\lambda}{1+\lambda} \right]^2 T^2, \quad (17)$$

where γ_{el} is defined by the electronic heat capacity per primitive cell (here atom),

$$\gamma_{\text{el}} = C_{\text{el}}/T = 2\pi^2 N(0)(1+\lambda)k_B^2/3n_{\text{ion}}.$$

The only material parameters in this result are λ and γ_{el} . Note that τ^{-1} is quadratic in λ in the weak-coupling limit, and linear for strong coupling. Of course the Coulomb interaction will become important as λ is reduced. This formula is a factor of $2(1+\lambda)$ less than the one derived by Allen and Silberglitt,³ the factor of 2 from the inclusion of exchange [Fig. 1(c)].

As mentioned earlier, Eq. (17) may be derived from a single approximation, namely the one leading to Eq. (16) for τ_{ex}^{-1} . Having arrived at this approximation in steps, however, we can argue (see Appendix) that these tend to counteract each other, so that this result is probably neither an upper nor lower bound on the exact τ^{-1} . Beyond these mathematical approximations, the neglect of the Coulomb contribution probably overestimates τ^{-1} , although the results of Ref. 4 suggest that this may be a small effect for at least some cases with $\lambda \gtrsim 0.4$.

The electron-electron contribution to the electrical resistivity is related to the quasiparticle decay rate [Eqs. (5) and (6)] in a simple manner, assuming that the total resistivity is dominated by an elastic scattering mechanism that fixes the nonequilibrium distribution in the usual relaxation time form. The relation is²⁸

$$\rho = \frac{1}{e^2} \left[\frac{m}{n} \right]_{\text{eff}} \tau^{-1} (1+\lambda) \Delta = 4\pi \Omega_p^{-2} \tau^{-1} (1+\lambda) \Delta, \quad (18)$$

where the plasma frequency Ω_p is defined by a Fermi surface average of the electron velocity, $\Omega_p^2 = e^2 \langle |\mathbf{v}_k|^2 \rangle / [3\pi^2 N(0)]$; and the parameter Δ , called the fractional umklapp scattering, is a more complicated

average²⁹ involving initial and final velocities in scattering events ($\mathbf{v}_1, \mathbf{v}_2$ and $\mathbf{v}_3, \mathbf{v}_4$, respectively),

$$\Delta = \langle |\mathbf{v}_1 + \mathbf{v}_2 - \mathbf{v}_3 - \mathbf{v}_4|^2 \rangle \langle |2\mathbf{v}_k|^2 \rangle^{-1},$$

in this case weighted by the scattering probability. Now Ω_p has been calculated for most of the metallic elements,^{30,31} but Δ for only a few, and only for Al among cases studied here. So we rely on the quasiparticle decay rate for a more direct quantitative test of the theory, and include the electrical resistivities more qualitatively.

III. RESULTS AND COMPARISON WITH EXPERIMENT

Focusing initially on the quasiparticle decay rate, we list on Table II the values of the coefficient

$$\alpha = \tau^{-1} T^{-2} \quad (19)$$

computed with Eq. (17) for a representative set of elements with $\lambda \geq 0.3$ and compare these with experimental values where available. The experimental entries in some cases represent a range of values arising from anisotropy and/or experimental uncertainty. Individual sources are listed on Table III and will be discussed shortly. The agreement is surprisingly good quantitatively, especially given the simplicity of Eq. (17).

With the exception of Nb, experimental data are available only in the weak-coupling cases $\lambda \lesssim \frac{1}{2}$. The larger α -values are not readily observable because the ratio of the superconducting transition temperature T_c to the Debye temperature $\Theta_D = \omega_D$ is large (see columns 5 and 6 of Table II). For $T > T_c$ the electron-phonon contribution ($\sim T^3$ or faster) dominates the electron-electron. To observe α with $T < T_c$ requires sufficiently high magnetic fields to suppress superconductivity. For example, in Nb (one of the best strong-coupling candidates) the data are found only for $T < T_c$ and in magnetic fields $\sim kG$. This allows for the use of magnetoacoustic attenuation, but rules out the more accurate radio frequency size effect technique, which has provided most of the other quasiparticle data (Table III). Among other strong-coupling elements, judging from Table II, V is probably the most favorable candidate, Ta less favorable, and Pb, La, and Hg very unfavorable for observing electron-electron scattering. The best candidate overall appears to be Ru, with Os, Mo, and Re close behind. The simple metals Al, Ga, and Zn appear to be reasonable candidates as well.

We have considered signatures of electron-electron processes in the superconducting phase,³² which will be discussed in a future publication. We find that the best candidates in the normal phase tend also to be the best candidates in the superconducting phase.

Although the α values are clustered around 0.4–0.5, the γ_{el} values range over an order of magnitude, and so we plot the results as a function of this parameter on Fig. 4. The experimental points for Al, Os, and Ru are inferred from electrical resistivity data as will be discussed. The data are consistent with the predicted linear dependence on γ_{el} [or $N(0)$]. This contrasts with the quadratic dependence found in a calculation²² of Coulomb scatter-

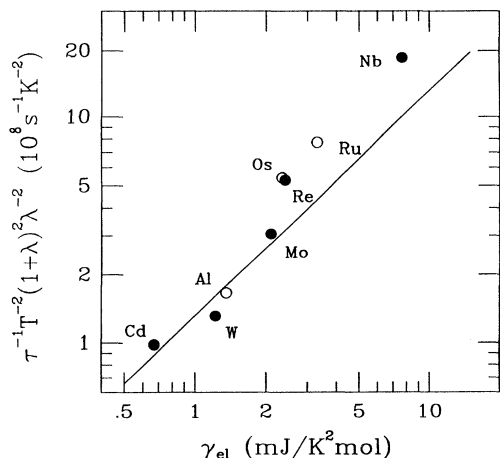


FIG. 4. Phonon-mediated electron-electron scattering rate with explicit λ dependence removed, plotted vs the coefficient of the electronic heat capacity. The solid line represents Eq. (17), the filled circles represent quasiparticle data (Table II), and the open circles represent electrical resistivity data as described in the text.

ing in the s - d model, in which the conducting s -electrons scatter from the more massive d electrons. Although the s - d model is now known not to apply to most transition-metal Fermi surfaces, which are highly hybridized, the quadratic dependence indeed seems to apply to magnetic metals,²² and presumably reflects in some way the importance of the underlying Coulomb interaction for quasiparticle decay in those cases. It would be interesting to obtain quantitative estimates from a different microscopic approach, for example, along the lines of Ref. 33, appropriate to the magnetic case. Neither the quasiparticle data nor the electrical resistivity data shown here are described as well by a quadratic dependence.

Let us discuss the entries in Table III individually.

A. Cd

The experimental data for Cd are obtained from the radio-frequency size effect (RFSE). The smaller value of α (Ref. 34) applies to a limiting-point orbit near the cap of the third-zone lens of the Fermi surface. The larger value³⁵ applies to two extremal orbits, also on the lens.

TABLE II. Coefficient α of the phonon-mediated electron-electron scattering rate calculated from Eq. (17) using parameters λ and γ_{el} , with the molar values of γ_{el} first divided by Avogadro's number. Experimental α values, in some cases averages, are from quasiparticle data as detailed in Table III. Values in parentheses are inferred from electrical resistivity data as described in the text. The Debye temperature Θ_D and superconducting transition temperature T_c are tabulated only to identify good and bad candidates for observable electron-electron scattering effects.

	λ^a	$(\text{mJ}/\text{mol K}^2)$ γ_{el}^b	$(10^7 \text{ s}^{-1} \text{ K}^{-2})$ α_{th}	α_{exp}	(K) Θ_D^b	(K) T_c^b
Al	0.43	1.36	1.6	(1.5)	423	1.2
Ga	0.4	0.60	0.65		317	1.09
Sn	0.72	1.78	4.1		196	3.72
In	0.81	1.70	4.5		109	3.40
Pb	1.55	3.14	15		102	7.23
Zn	0.42	0.64	0.74		316	0.88
Cd	0.40	0.67	0.73	0.8	252	0.56
Hg	1.6	2.2	11		75	4.15
Tl	0.80	2.83	7.3		88	2.36
Mo	0.40	2.10	2.3	2.5	459	0.92
Ir	0.35	3.15	2.8		425	0.10
W	0.3	1.22	0.86	0.7	388	0.012
V	0.6	9.04	17		399	5.38
Nb	1.1 ^c	7.66	28	51	277	9.26
Ta	0.88 ^c	5.84	17		258	4.48
La	0.85	10.1	28		142	6.0
Ru	0.4	3.3	3.6	(6.2)	600	0.51
Os	0.4	2.35	2.5	(4.4)	500	0.66
Ti	0.35	3.41	3.0		426	0.39
Re	0.45	2.40	3.1	5.1	415	1.7
Tc	0.7	4.06	9.1		351	7.77
Zr	0.4	2.91	3.1		289	0.52

^aReference 24, except as noted.

^bFrom compilation of G. Gladstone *et al.*, in *Superconductivity*, edited by R. D. Parks (Dekker, New York, 1969), Vol. 2, Chap. 13.

^cP. B. Allen *et al.*, Phys. Rev. B **34**, 4331 (1986).

TABLE III. Sources of quasiparticle data are listed: Radio frequency size effect (RFSE), magnetoacoustic attenuation (MA), and Doppler-shifted cyclotron resonance (DSCR).

	$(10^7 \text{ s}^{-1} \text{ K}^{-2})$			
	α_{th}	α_{exp}		
Cd	0.73	0.6	RFSE	(Ref. 34)
		0.8	RFSE	(Ref. 35)
Mo	2.3	4.4	MA	(Ref. 41)
		2.4–2.9	DSCR	(Ref. 40)
		1.3–2.5	RFSE	(Ref. 37)
W	0.86	0.55–1.1	RFSE	(Ref. 42 and Ref. 43)
Nb	28	51	MA	(Ref. 41)
Re	3.1	4.3–6.2	RFSE	(Ref. 45)

The more accurate later data are consistent with the earlier value within its experimental uncertainty, suggesting that α is nearly isotropic over the lens piece of the Fermi surface. Large apparent T^2 terms were found on first- and second-zone orbits in the earlier work, but these were later found³⁵ to revert to T^3 dependence at lower temperatures. This behavior is understood theoretically^{36,35} to arise from electron-phonon scattering near cusplike regions of the orbit, where the Fermi surface has a small momentum gap $\Delta k < k_B T/c_s$, with c_s the speed of sound.

B. Mo

The RFSE data³⁷ are the most informative in this case: Measurements on many extremal orbits on the electron jack and hole octahedron indicate a nearly isotropic value (2.5) of α on these sheets. The smaller values 1.3 and 1.9 were found on the small hole ellipsoids. It is noted that these latter values are less reliable because the T^2 behavior is observable over a narrower temperature range, and furthermore the overlap of cyclotron resonance signals from spheroids and ellipsoids hampers the determination of the cyclotron effective mass. A critique is given of earlier RFSE work^{38,39} in which different values were found on the hole ellipsoids, but similar values on the larger sections. The Doppler-shifted cyclotron resonance (DSCR) technique⁴⁰ yields averages over noncentral orbits corresponding to extrema of dS/dk_z , where S is the area of an orbit with normal along the k_z axis. This entry represents two additional orbits on the electron jack and hole octahedron sections. The magnetoacoustic attenuation (MA) entry⁴¹ represents a single orbit in the (100) plane of the hole octahedron. Its value (4.4) is inconsistent with the other data. We choose 2.5 as a rough estimate of the average value of α .

C. W

The single entry in this case refers to the most recent RFSE work,^{42,43} where one can find a critique of earlier

RFSE work.^{38,39,44} As in Mo, α was found to be approximately isotropic on the electron jack and hole octahedron sections, with values between 0.55 and 0.65. The larger value 1.1 was found on the electron spheroid.

The case of W is interesting because a microscopic calculation of the Coulomb scattering rate was done by Potter and Morgan,²³ taking into account repeated scattering on a realistically shaped Fermi surface with tight-binding electron states. Pointwise values of α were calculated in the range 0.87–1.34 ($10^7 \text{ s}^{-1} \text{ K}^2$), with an average value (about 1.0) only slightly higher than the experimental average. It seems plausible that W, with $\lambda \sim 0.3$, is a borderline case in which Coulomb and phonon-mediated interactions are comparable. Although they would be expected to cancel somewhat, the cancellation would not be complete, owing both to different partial wave decompositions of the differential cross sections, and to different anisotropies of the total cross sections for the two contributions. It is possible that the magnitudes of the Coulomb and phonon-mediated interactions found in Ref. 23 and the present work (Table II), respectively, are both consistent with the experimental value.

D. Nb

The single entry in this case⁴¹ is from magnetoacoustic data on the extremal (100) orbit of the hole octahedron, analogous to the MA measurement in Mo. In both cases, the measured value of α is about twice the theoretical value. RFSE data are unavailable because of the high superconducting critical magnetic field in Nb.

E. Re

The range of α values quoted here represents RFSE data⁴⁵ for six orbits on the eighth-zone section of the Fermi surface. This section was chosen for the measurements because it is centered at the Γ point, so that electron-phonon scattering, being predominantly normal, is less severe here than on the other sections. Even so, a T^3 contribution to τ^{-1} (presumably from normal events) is clearly evident on three of the six orbits. The electron-electron contribution to τ^{-1} is isotropic within experimental uncertainty on this branch of the Fermi surface, while the electron-phonon contribution is highly anisotropic.

F. Electrical resistivity

Theoretical results for the resistivity parameter

$$A = \rho T^{-2} = 4\pi\Omega_p^{-2}\Delta(1+\lambda)\alpha \quad (20)$$

[see Eqs. (18) and (19)] are evaluated and compared with experimental values on Table IV. Direct comparison is possible only for Al, where the umklapp parameter Δ has been computed. Note that Ω_p is approximately uniform across the transition metals, so that A is approximately linear in γ_{el} , as mentioned earlier.

TABLE IV. Theoretical and experimental electrical resistivity coefficients A_{th} and A_{exp} . A_{th} is calculated using Eq. (20) with tabulated values of the plasma frequency Ω_p , Δ_{th} for Al (Ref. 29), and the values of λ and α_{th} from Table II. Other theoretical Δ values are not known. Apparent values Δ_{app} are inferred from A_{exp} and α_{exp} , the latter from Table II.

	(eV)	$(10^{-14} \Omega \text{ m K}^{-2})$		Δ_{th}	Δ_{app}
	Ω_p^a	A_{th}	A_{exp}^b		
Al	12.4	0.30	0.28 ^c	0.40	
Mo	8.1	2.4 Δ	1.3		0.5
W	7.4	1.0 Δ	0.5 ^d		0.6
Nb	9.1	35 Δ	2.3		0.04
Ru	8.9	3.1 Δ	2.7		
Os	8.7	2.3 Δ	2		
Re	7.4	4.0 Δ	4.5		0.6

^aReference 30 (first four), and Ref. 31 (last three).

^bT. L. Ruthruff, C. G. Grenier, and R. G. Goodrich, Phys. Rev. B **17**, 3070 (1978) except as noted.

^cReference 14.

^dReference 42.

G. Al

The close agreement in this case may be fortuitous. The more detailed theoretical treatment described in Ref. 4 results in a value about 40% larger, which is within the theoretical uncertainty of the present estimate. It is possible that the computed value of Δ is too large, and that a smaller value would bring the Ref. 4 value into closer agreement. A more detailed calculation along the lines of Ref. 46 would be informative, as would be new experimental quasiparticle data on Al.

Existing RFSE (Ref. 47) and surface Landau-level resonance⁴⁸ data show no evidence of electron-electron scattering; only the T^3 dependence expected from electron-phonon scattering is resolved. New RFSE experiments are being undertaken⁴⁹ which extend the temperature range and precision of previous measurements. A T^2 coefficient consistent with the electrical resistivity data should be observable in these experiments.

H. Mo, W, Re, and Nb

In these cases where both resistivity and quasiparticle data are available, we infer "apparent" values of the umklapp parameter (Δ_{app} in column 5) from Eq. (20) using experimental values of A_{exp} and α_{exp} (we use the averaged α values shown in Table II). Values near $\Delta \sim \frac{1}{2}$ seem plausible, based on computed values for Al (Ref. 29) and Pb (Ref. 4) (both 0.4), so that the experimental values of A_{exp} and α_{exp} appear consistent for Mo, W, and Re, but not for Nb. The Nb resistivity data were also found at $T < T_c$ and therefore in high magnetic fields, requiring subtraction of the magnetoresistivity in order to determine A_{exp} .

I. Ru and Os

Since quasiparticle data are unavailable in these cases, and since Δ has not been calculated, we must assume a value of Δ in order to compare theory and experiment. Taking $\Delta \sim \frac{1}{2}$ based on calculated values for Al and Pb and the empirical values Δ_{app} for Mo, W, and Re, the discrepancy is within about a factor of 2. It is unlikely that Δ is significantly larger than $\frac{1}{2}$, as would be required for perfect agreement. The "experimental" points for Ru and Os in Fig. 1 are obtained using this value.

J. A 15 compounds

Many compounds exhibit T^2 dependence in their low-temperature resistivities. This effect has received much attention in the A 15 compounds where those with high T_c (~ 20 K) show a large effect (above T_c) and those with low T_c show little or no such effect.^{50,10} Estimates based on the Coulomb interaction, as considered in Ref. 22, fall two orders of magnitude below the larger observed T^2 terms.^{51,52} Estimates based on the present treatment of the phonon-mediated interaction, taking eight atoms per primitive cell, improve the agreement by one order of magnitude. It seems unlikely that anisotropy and phonon softening could by themselves account for the remaining discrepancy, although they move things in the right direction. So this result does not remove the motivation to look beyond the Migdal-based formalism, as done for example in Ref. 53.

IV. SUMMARY

Starting with an exact formulation of the inelastic quasiparticle decay rate, we have derived a simple approximate formula for the phonon mediated electron-electron contribution at low temperatures. The result, $\tau^{-1}/T^2 \sim \gamma_{el}\lambda^2/(1+\lambda)^2$, is quadratic in λ for weak coupling, and linear for strong coupling. Nevertheless, the best candidates for observation of this effect among metal elements are weak-coupling superconductors ($\lambda \sim 0.5$) with high Debye temperatures. Strong-coupling elements tend to have large values of the ratio T_c/Θ_D , which means that electron-phonon scattering dominates electron-electron for $T > T_c$.

The available experimental data among superconducting elements agree quantitatively with this formula, and in particular they confirm the predicted linearity in γ_{el} , which varies by more than an order of magnitude in the available cases. It is notable that this range includes simple metals and transition metals, so that the distinction regarding the phonon-mediated interaction is only a quantitative one, measured primarily by $N(0)$, or γ_{el} . The linear dependence predicted here for τ^{-1} (and also approximately for ρ) contrasts with the quadratic dependence on γ_{el} associated with magnetic metals.

We would not argue that the Coulomb contribution is negligible in all the cases studied here. Although MacDonald⁴ found it to be negligible in Al (and Pb), Potter and Morgan²³ found it to be important in W, which with $\lambda \sim 0.3$ we consider to be a borderline case. However, the

agreement found in eight metals (in three cases with both quasiparticle and electrical resistivity data) argues that the phonon-mediated interaction is generally at least as important as the Coulomb interaction for quasiparticle decay in the superconducting elements, and although this interaction is complicated in detail, the resulting values of τ^{-1} are given to surprising accuracy by a simple expression.

ACKNOWLEDGMENTS

It is a pleasure to thank Phil Allen and Michael Reizer for many informative discussions. This work was supported in part by the DOE—Basic Energy Sciences, Division of Materials Research.

APPENDIX

We suggest here an approach for computing the exact τ^{-1} , and then argue that Eq. (9) probably overestimates the exact result, but that subsequent approximations probably underestimate Eq. (9). So the final result is probably neither an upper nor a lower bound on the exact result.

According to Eq. (5), we may interchange the \mathbf{k} and \mathbf{q} integrals to show that τ^{-1} may be computed as a Brillouin zone sum of a function (of \mathbf{q}), which is itself computed as a double integral over the cylinder shown schematically in Fig. 3. Each cylinder integral is of the type [Eq. (7)]. The *direct* part τ_d^{-1} may be computed more simply by defining the matrix

$$U_{\sigma\sigma'}(\mathbf{q}) = 2\pi \sum_{\mathbf{p}} \delta(Z\epsilon_{\mathbf{p}})\delta(Z\epsilon_{\mathbf{p}+\mathbf{q}})g_{\sigma}(\mathbf{p}+\mathbf{q},\mathbf{p}) \times g_{\sigma'}(\mathbf{p}+\mathbf{q},\mathbf{p})(\omega_{\mathbf{q}\sigma}\omega_{\mathbf{q}\sigma'})^{-(1/2)}, \quad (\text{A1})$$

in terms of which

$$\tau_d^{-1} = \frac{8\pi(k_B T)^2}{3N(0)Z(0)} \sum_{\mathbf{q}} \text{Tr} U^2(\mathbf{q}). \quad (\text{A2})$$

The \mathbf{q} integrand here involves just a single cylindrical in-

tegration. These two equations may be compared with Eqs. (8) and (9); the left-hand side of Eq. (8) [later called $Q(\mathbf{q})$ in Eq. 12], is equal to $\text{Tr} U(\mathbf{q})$. So Eq. (9) is similar to (A2), but its integrand is $[\text{Tr} U(\mathbf{q})]^2$.

The ratio of Eq. (9) to Eq. (A2) would take on its maximum value, the dimension of U (i.e., the number of phonon modes) if and only if $U \sim I$. This is impossible, however, because it would require that all the off-diagonal elements vanish, which none of them do, in general. An approximation which is probably much closer to the truth is $U_{\sigma\sigma'}(\mathbf{q}) = f_{\sigma}(\mathbf{q})f_{\sigma'}(\mathbf{q})$, which follows for example if the integrand of $U(\mathbf{q})$ is independent of the cylinder integration variable \mathbf{p} . In this approximation the ratio of Eq. (9) to (A2) is unity. This would be the minimum value if U were positive definite, which seems likely but is not guaranteed as far as we know. Therefore it seems likely that Eq. (9) overestimates τ_d^{-1} .

The next approximation is to assume that $Q(\mathbf{q}) \sim q^{-1}$ (and is isotropic) in Eqs. (13) and (14). This approximation makes $C[Q(\mathbf{q})] = \frac{4}{3}$ [Eq. (15)], only slightly above the absolute minimum (unity), which is achieved according to Schwartz inequality if and only if $Q(\mathbf{q}) = \text{constant}$ (which is unphysical). Angular dependence would only increase C ; radial dependence could increase or decrease it depending for example upon whether $qQ(q)$ were a monotonically decreasing or increasing function, respectively. It is likely that this approximation, being close to the minimum, produces an underestimate of τ_d^{-1} as given by Eq. (9).

Finally, the approximation for exchange ($R \equiv \tau_d |\tau_{\text{ex}}^{-1}| \rightarrow \frac{1}{2}$) [Eq. (16)], maximizes R and thus underestimates the total scattering rate. This may be seen from Eq. (5) by combining the exchange term with half the direct term in the form of a perfect square (whose minimum is zero). The same limit is achieved for example when nearly free electrons undergo purely s -wave scattering. For comparison, the Thomas Fermi screened Coulomb potential produces values around 0.4. The microscopic calculation⁵ of the phonon-mediated interaction in alkali metals finds R at least this far below $\frac{1}{2}$.

*Deceased.

†Permanent address: Department of Physics, Dartmouth College, Hanover, NH 03755.

¹This point was first made by Migdal (Ref. 2), and later developed by T. Holstien, Ann. Phys. (N.Y.) **29**, 410 (1964), and by Allen and Silbergliitt (Ref. 3). Quantitative estimates of the effect of the phonon-mediated interaction in combination with the Coulomb interaction were first made by MacDonald (Ref. 4).

²A. B. Migdal, Zh. Eksp. Teor. Fiz. **34**, 1438 (1958) [Sov. Phys. JETP **7**, 996 (1958)].

³P. B. Allen and R. Silbergliitt, Phys. Rev. B **9**, 4733 (1974).

⁴A. H. MacDonald, Phys. Rev. Lett. **44**, 489 (1980).

⁵A. H. MacDonald, R. Taylor, and D. J. W. Geldart, Phys. Rev. B **23**, 2718 (1981).

⁶A. H. MacDonald and D. J. W. Geldart, J. Phys. F **10**, 677 (1980).

⁷J. M. B. Lopes dos Santos and D. Sherrington, J. Phys. F **13**,

1233 (1983).

⁸J. M. B. Lopes dos Santos and D. Sherrington, J. Phys. F **14**, 2039 (1984).

⁹K. Schwartzman and W. E. Lawrence, Phys. Rev. B **37**, 1136 (1988).

¹⁰M. Kaveh and N. Wiser, Adv. Phys. **33**, 257 (1984).

¹¹R. J. M. van Vucht, H. van Kempen, and P. Wyder, Rep. Prog. Phys. **48**, 853 (1985).

¹²B. Levy, M. Sinvani, and A. J. Greenfield, Phys. Rev. Lett. **43**, 1822 (1979).

¹³C. W. Lee *et al.*, Phys. Rev. B **25**, 1411 (1982).

¹⁴J. H. J. M. Ribot, J. Bass, H. van Kempen, R. J. M. Van Vucht, and P. Wyder, J. Phys. F **9**, L117 (1979); Phys. Rev. B **23**, 532 (1981).

¹⁵P. A. Schroeder, B. Blumenstock, V. Heinen, W. P. Pratt, Jr., and S. Steenwyck, Physica **107B**, 137 (1981).

¹⁶Electron-electron scattering is observable in some metals at high temperatures because it violates the Wiedemann-Franz

- Law, while the competing electron-phonon mechanism, being effectively elastic, obeys it (see Ref. 21 for discussion).
- ¹⁷J. G. Cook, M. P. Van Der Meer, and M. J. Laubitz, *Can. J. Phys.* **50**, 1386 (1972); J. G. Cook, *ibid.* **57**, 871 (1979); **57**, 1216 (1979); **60**, 1759 (1982).
- ¹⁸M. Khoshnevisan, W. P. Pratt, Jr., P. A. Schroeder, S. Steenwyk, and C. Uher, *J. Phys. F* **9**, L1 (1979); *Phys. Rev. B* **19**, 3873 (1979).
- ¹⁹S. D. Steenwyk, J. A. Rowlands, and P. A. Schroeder, *J. Phys. F* **11**, 1623 (1981).
- ²⁰R. Stubi, P.-A. Probst, R. Huguenin, and V. A. Gasparov, *J. Phys. F* **18**, 1211 (1988).
- ²¹M. J. Laubitz, *Phys. Rev. B* **2**, 2252 (1970).
- ²²M. J. Rice, *Phys. Rev. Lett.* **20**, 1439 (1968).
- ²³C. Potter and G. J. Morgan, *J. Phys. F* **9**, 493 (1979).
- ²⁴G. Grimvall, *Phys. Scr.* **14**, 63 (1976).
- ²⁵A. I. Akhiezer, A. I. Akhiezer, and V. G. Baryakhtar, *Phys. Lett.* **44A**, 323 (1973).
- ²⁶P. B. Allen, *Phys. Rev. B* **6**, 2577 (1972).
- ²⁷About half of the cases we consider have hexagonal structure, with two atoms per primitive cell. Since the band gap is small or zero over the first Brillouin-zone boundary, it seems appropriate to use the Jones zone description which doubles the Brillouin-zone volume, counts all phonon modes within acoustic branches, and makes n_{ion} in Eqs. (13) and (17) the actual atomic density.
- ²⁸G. R. Parkins, W. E. Lawrence, and R. W. Christy, *Phys. Rev. B* **23**, 6408 (1981).
- ²⁹W. E. Lawrence and J. W. Wilkins, *Phys. Rev. B* **7**, 2317 (1973).
- ³⁰P. B. Allen, *Phys. Rev. B* **36**, 2920 (1987).
- ³¹B. A. Sanborn, P. B. Allen, and D. A. Papaconstantopoulos, *Phys. Rev. B* **40**, 6037 (1989).
- ³²K. Schwartzman and W. E. Lawrence, in *Proceedings of the 17th International Conference on Low Temperature Physics*, edited by U. Eckern *et al.* (North Holland, Amsterdam, 1984), Vol. II, p. 1055; K. Schwartzman, Ph.D. thesis, Dartmouth College, 1984, available from University Microfilms, Ann Arbor, MI.
- ³³M. Yu. Reizer, *Phys. Rev. B* **39**, 1602 (1989).
- ³⁴P.-A. Probst, W. M. MacInnes, and R. Huguenin, *J. Low Temp. Phys.* **41**, 115 (1980).
- ³⁵A. Jaquier, P.-A. Probst, R. Stubi, R. Huguenin, and W. E. Lawrence, *J. Phys. Condens. Matter* **3**, 10065 (1992).
- ³⁶W. E. Lawrence, Wei Chen, and J. C. Swihart, *J. Phys. F* **16**, L49 (1986).
- ³⁷M. A. Arutyunyan and V. A. Gasparov, *Zh. Eksp. Teor. Fiz.* **76**, 369 (1979) [*Sov. Phys. JETP* **49**, 188 (1979)].
- ³⁸V. V. Boiko, V. F. Gantmakher, and V. A. Gasparov, *Zh. Eksp. Teor. Fiz.* **65**, 1219 (1973) [*Sov. Phys. JETP* **38**, 604 (1974)].
- ³⁹V. A. Gasparov, in *Proceedings of the EPS Study Conference, Cavtat, Yugoslavia*, edited by B. Leontić, E. Babić, and R. Krsnik (Sveučilišna Naklada Liber, Zagreb, 1977).
- ⁴⁰V. A. Gasparov, I. F. Voloshin, and L. M. Fisher, *Solid State Commun.* **29**, 43 (1979).
- ⁴¹J. A. Rayne and J. R. Leibowitz, *J. Phys. (Paris) Colloq.* **39**, C6 (1978).
- ⁴²J. van der Maas, R. Huguenin, and V. A. Gasparov, *J. Phys. F* **15**, L271 (1985).
- ⁴³I. F. Voloshin, V. A. Gasparov, S. V. Kravchenko, and L. M. Fisher, *Zh. Eksp. Teor. Fiz.* **92**, 745 (1987) [*Sov. Phys. JETP* **65**, 419 (1987)].
- ⁴⁴B. P. Nilaratna and S. Myers, *J. Phys. Paris Colloq.* **39**, C6 (1978).
- ⁴⁵C. A. Steele and R. G. Goodrich, *J. Phys. F* **10**, 873 (1980).
- ⁴⁶J. E. Black, *Can. J. Phys.* **56**, 708 (1978).
- ⁴⁷V. A. Gasparov and M. H. Harutunian, *Solid State Commun.* **19**, 189 (1976).
- ⁴⁸T. Wegehaupt and R. E. Doezema, *Phys. Rev. B* **18**, 742 (1978).
- ⁴⁹A. Jaquier *et al.* (private communication).
- ⁵⁰M. Gurvitch, *Phys. Rev. Lett.* **56**, 647 (1986).
- ⁵¹M. Gurvitch, A. K. Ghosh, H. Lutz, and M. Strongin, *Phys. Rev. B* **22**, 128 (1980).
- ⁵²G. S. Knapp, S. D. Bader, and Z. Fisk, *Phys. Rev. B* **13**, 3783 (1976).
- ⁵³C. C. Yu and P. W. Anderson, *Phys. Rev. B* **29**, 6165 (1984).